Iranian Journal of Materials Science and Engineering, Vol. 20, Number 1, March 2023
RESEARCH PAPER

Resonance Phenomenon and Structural Properties of Fe Substituted PZT Ceramics Prepared by the Sol-Gel Method

Ahabboud Malika*, Gouitaa Najwa, Fatima Zahra Ahjyaje, Lamcharfi Taj-dine, Abdi Farid

* *malikasmp2013@gmail.com*

Signals, Systems and Components Laboratory (LSSC), Electrical Engineering Department, University Sidi Mohamed Ben Abdellah, FST Fez, Imouzzer Road B.P. 2202, Morocco

Received: August 2022 **Revised: March 2023** **Accepted: March 2023**
DOI: 10.22068/ijmse.2938

Abstract: *In this paper, $Pb_{1-x}Fe_x(Zr_{0.52}Ti_{0.48})O_3$ (PFZT) nano-size powders, in which x changed from 0.00 up to 0.20, were synthesized, using the sol-gel method. The PFZT samples were characterized by X-ray diffraction (XRD), Raman spectroscopy, scanning electron microscopy (SEM), and impedance spectroscopy. According to the experimental results, a combination of rhombohedral and tetragonal symmetries was seen in all the samples. The SEM investigation indicated that the grains were homogeneous with regular morphology, and the average grain size changed with Fe concentration. The dielectric characterizations showed that the dielectric permittivity increases with increasing temperature, and the Fe amount shifts down the temperature of transition. Moreover, a dielectric resonance phenomenon is observed for all the PFZT ceramics.*

Keywords: *$Pb_{1-x}Fe_x(Zr_{0.52}Ti_{0.48})O_3$, X-ray diffraction, Raman spectroscopy, Sol-gel, dielectric permittivity, resonance.*

1. INTRODUCTION

Lead zirconate titanate $PbZr_xTi_{1-x}O_3$ (PZT) is an ABO_3 perovskite oxide type. These compounds display a multitude of properties (ferroelectric, magnetic piezoelectric...) and are extensively used in practical devices (piezoelectric, electrostrictive, pyroelectric electro-optic, and magnetoelectric, etc). PZT is among the most investigated ferroelectric materials, due to its various applications such as sensors, actuators microelectronic devices, infrared detectors, non-volatile ferroelectric memory devices, and accelerometers [1, 2], and microelectromechanical systems (MEMS) [3]. All these applications are intensively linked to the physical properties of the material, especially piezoelectric and ferroelectric ones.

PZT material can be synthesized by several physicals, chemicals, and mechanical methods such as solid-state [3, 4], sol-gel [5, 6], hydrothermal [7], coprecipitation method, and others [8, 9]. However, although PZT ceramics have good dielectric, piezoelectric, and electromechanical properties [10, 11] these characteristics are generally improved by varying the Zr/Ti ratio, or by substituting cations on A site (replacing Pb^{2+}) or site B (replacing Zr^{4+} and/or Ti^{4+}). In this sense, much research has been conducted on Mn-doped PZT [12], La-doped PZT [13], and K-doped PZT [14]. On the other hand, PZT materials with a ratio Zr/Ti of about 52/48 ($PbZr_{0.52}Ti_{0.48}O_3$: PZT52) near the morphotropic phase boundary, corresponding to the coexistence of both the rhombohedral and tetragonal phases, are well known to present high piezoelectric and dielectric properties [5, 15, 16].

Moreover, it's known that in a ferroelectric perovskite structure ABO_3, substituting A and /or B cation with a magnetic ion leads to a multiferroic property combining ferroelectric and ferromagnetic properties, consequently, the magnetization can be switched with an applied electric field and vice versa the polarization by a magnetic field. This property can be very useful for random access memory elements, by switching magnetization by an applied electric field RAMs could operate at very low voltage values with fast and non-destructive Write/ Read operations.

However, most known multiferroics (such as terbium manganites $TbMnO_3$ or $TbMn_2O_5$) switch only a few nC/cm^2 with applied magnetic fields too small for reliable discrimination between "1" and "0" states [17], [18]. Moreover, they operate only at cryogenic temperatures. $BiFeO_3$ might operate at room temperature, but its magnetism is very weak and it neither permits switching large magnetizations with electric fields nor large polarizations with magnetic fields [17],

[DOI: 10.22068/ijmse.2938]

[19], [20]. PZT as a composite with ferrite was already investigated as a multiferroic [21, 22].
However, these sintered ceramic composites had lower Magneto-Electric (ME) coefficients. An important step in multiferroic materials was the development of rare-earth-iron-based composites with relatively high ME [23-26]. Although many different compound families have been widely investigated as multiferroic ME materials, high inherent coupling between multiferroic order parameters (especially above room temperature) has not yet been found in a single-phase compound. Hence, in this paper, we are interested in the synthesis and characterization of $Pb_{(1-x)}$ Fe_x $(Zr_{0.52}Ti_{0.48})O_3$, we are interested in the structural and dielectric study of these ceramics.
Doping PZT with transition metals like Fe also helped it develop ferromagnetic characteristics. These doped materials and ferromagnetism are produced as a result of oxygen vacancies and hybridization of the p and d orbitals of the O and Fe atoms [27] There are only a few studies related to PZT-doped Fe compounds reported in the literature. The doped acceptor ions such as Fe present a high p-type electrical conductivity, a decrease in dielectric constant, an increase in frequency constant, and electromechanical properties [28, 29]. Some researchers have tried to study the properties of Fe-doped PZT. For example, Kumari et al. reported that the crystallite size of PZT ceramics decreases with an increase in the Fe dopant ratio [30]. This effect decreased the ferroelectric polarization and increased the magnetization. Sangawar et al. synthesized Fe-doped PZT materials by solid-state method and they studied the effect of sintering temperature on the dielectric and piezoelectric properties of these materials [31]. Samanta et al. fabricated Fe-doped PZT ceramics by the sol–gel process [32]. They reported that the unit cell volume of the samples decreased with subsequent Fe doping. Li Jin reported the piezoelectric and mechanical properties of PZT doped with Fe [10].

2. EXPERIMENTAL PROCEDURE

We have prepared our samples (PFZT) by the sol-gel method, using solutions of lead acetate trihydrate $(PbC_2H_3O_2)_2$ $3H_2O$), Zirconium Acetate $Zr(CH_3COO)_4$, titanium isopropoxide $Ti(OCH(CH_3)_2)_4$, and Iron II Acetate $Fe(C_2H_3O_2)_2$ as starting precursors. The first step is to stoichiometrically mix the solutions of these precursors according to the formula $Pb_{(1-x)}Fe_x$ $(Zr_{0.52}Ti_{0.48})O_3$ $(0.00 \leq x \leq 0.20)$ and stir them for one hour, forming a xerogel and then a gel. After drying it at 80°C, the obtained product is then ground using an agate mortar and calcined at 700°C for 4 hours. Ones the mentioned steps are done, the milled powders were compacted uniaxially under a pressure of about 7 tons/cm^2 to form pellets of 12 mm in diameter and 2 mm in thickness. The pellets were then sintered in an air atmosphere for 4 h at 1100°C. To limit the Pb volatilization which makes the material non-stoichiometric [33, 34]; the sintering was performed under a rich PbO atmosphere. The synthesized materials were characterized by X-ray diffraction (XRD) (XPERT- PRO with Cu Kα radiation with λ= 1.5406 Å, 2θ range 20°-70°), and fitted using Rietveld refinement in ″FullProf″ software. Raman spectroscopy was also studied and scanning electron microscopy (SEM) was used to study the morphology of the sintered pellets. The dielectric properties were studied as a function of temperature (up to 400°C) and frequency (up to 2MHz) using an Agilent impedance analyzer (Agilent E4980A).

3. RESULTS AND DISCUSSION

3.1. X-ray Diffraction

Fig .1.a shows the diffractograms of the powders (PFZT) (x= 0.00, 0.025, 0.05, 0.075, 0.10, 0.15, and 0.20) calcined at 700°C for 4 hours. The results of these diffractograms show that all PFZT powders crystallize in the pure perovskite phase without the presence of secondary phases. The zoom of the peak (110) in fig. 1.b, reveals no change in this peak position for x= 0.00 to 0.75 of Fe content. While at x= 0.10, we notice a displacement of this peak towards the higher angles. Beyond x= 0.10, the peak (110) fluctuates between x= 0.15 and x= 0.20. The shift of the peak (110) towards the higher angles can be attributed to the substitution of the Pb atom of ionic radius $r_i(Pb^{2+})$= 1.2 Å by an atom of smaller ionic radius $r_i(Fe^{2+})$= 0.76 Å). While the fluctuation observed may be due to the substitution of the Zr^{4+}/Ti^{4+} couple by Fe^{2+}.
The Rietveld refinement was performed using XRD data for PFZT powders (x= 0; 0.025; 0.05; 0.075; 0.10; 0.15 and 0.20). The results are shown

[DOI: 10.22068/ijmse.2938]

in fig .2. The refinement analysis of the samples indicates that all PFZT powders crystallize in two distinct phases; tetragonal and rhombohedral with space groups P4mm and R3m respectively without change in phase structure with Fe doping. The coexistence of the two phases during the insertion of the dopants in the PZT perovskite is in good agreement with the results of the literature [14, 35, 36]. The values of the lattice parameters of the PFZT powders, the reliability factor $\chi 2$, the R-parameters (Rp profile residual) and (Rwp weighted profile residual) as well as the percentages of the two phases (tetragonal and rhombohedral) as a function of the Fe content are shown in table 1. All the parameters are calculated using the Rietveld refinement method. These results show that the lattice parameters for the tetragonal and rhombohedral structure of PFZT samples are fluctuating; they decreased for certain values of x and increased for others. However, the decrease in the lattice parameters is attributed to the fact that the Fe with ionic radius $r_i(Fe^{2+})= 0.76$ Å, substitutes for another atom with a larger ionic radius (Pb of ionic radius $r_i(Pb^{2+})= 1.2$ Å). While the increase in lattice parameters may be due to the substitution of Ti ions with ionic radius $r_i(Ti^{4+})= 0.605$Å or Zr $r_i(Zr^{4+})= 0.72$Å lower than that of the Fe ion $r_i(Fe^{2+})= 0.76$ Å. On the other hand, we observed that R< 15.0 and $\chi^2 < 2.0$, for all the samples, which indicates a good crystallinity of the powders.

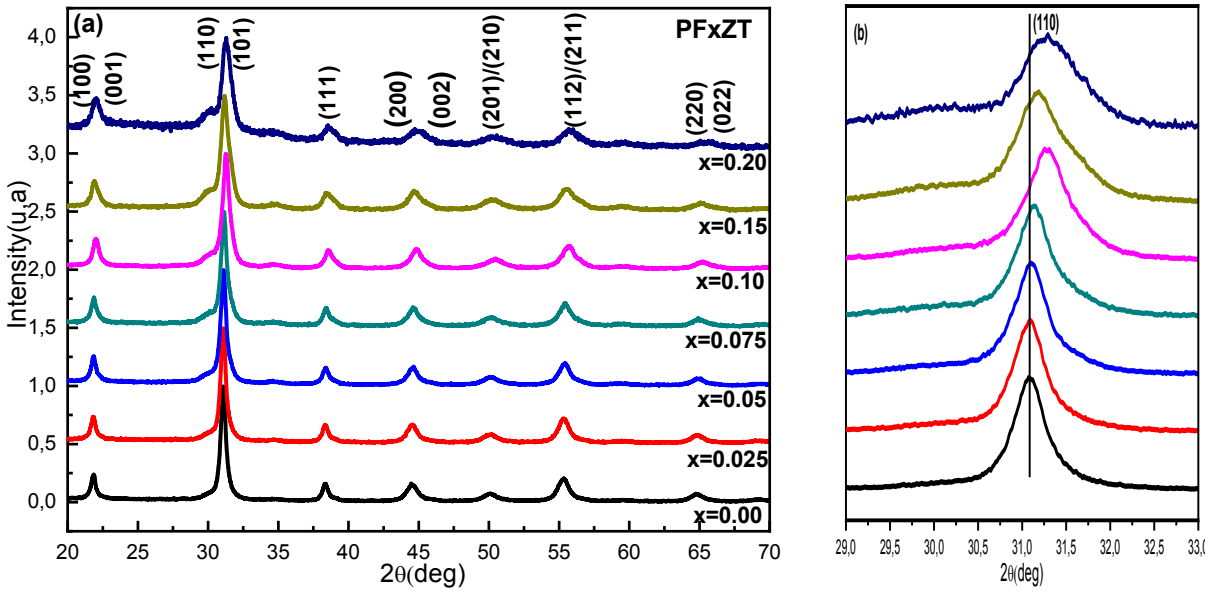

Fig. 1. . a. XRD patterns and b. Zoom of the peak (110) of $Pb_{(1-x)}$ $Fe_x(Zr_{0.52}Ti_{0.48})O_3$ samples ($0.00 \leq x \leq 0.20$), calcined at 700°C for 4h.

Table 1. Lattice parameters (a,c), Rp, RWP, and χ^2, values for the structures of PFZT ceramics for $0 \leq x \leq 0.20$.

x	Tetra		Rhom		Rp (%)	R_{wp}	χ^2
	Lattice parameters (a,c)	%	Lattice parameters (a,c)	%			
x=0.00	a=4.0402 c=4.1098	51.58	a= 5.7510 c=14.1262	48.42	3.92	4.97	1.12
x=0.025	a=4.0278 c=4.1212	39.44	a= 5.7451 c=14.1502	60.56	5.06	6.53	1.31
x=0.05	a= 4.0495 c= 4.0791	93.92	a= 6.0406 c=11.9728	6.08	4.35	5.69	1.59
x=0.075	a= 4.0512 c= 4.0783	91.67	a=5.76534 c=13.6599	8.33	5.48	6.98	1.34
x=0.10	a= 4.0250 c= 4.0690	82.57	a= 5.7087 c=14.0647	17.43	4.06	5.20	1.33
x=0.15	a= 4.0383 c= 4.0770	82.27	a= 5.7275 c=13.7447	17.73	5.20	6.54	1.30
x=0.20	a= 4.0137 c= 4.0793	87.91	a= 5.6890 c=14.1103	12.09	4.20	5.37	0.80

[DOI: 10.22068/ijmse.2938]

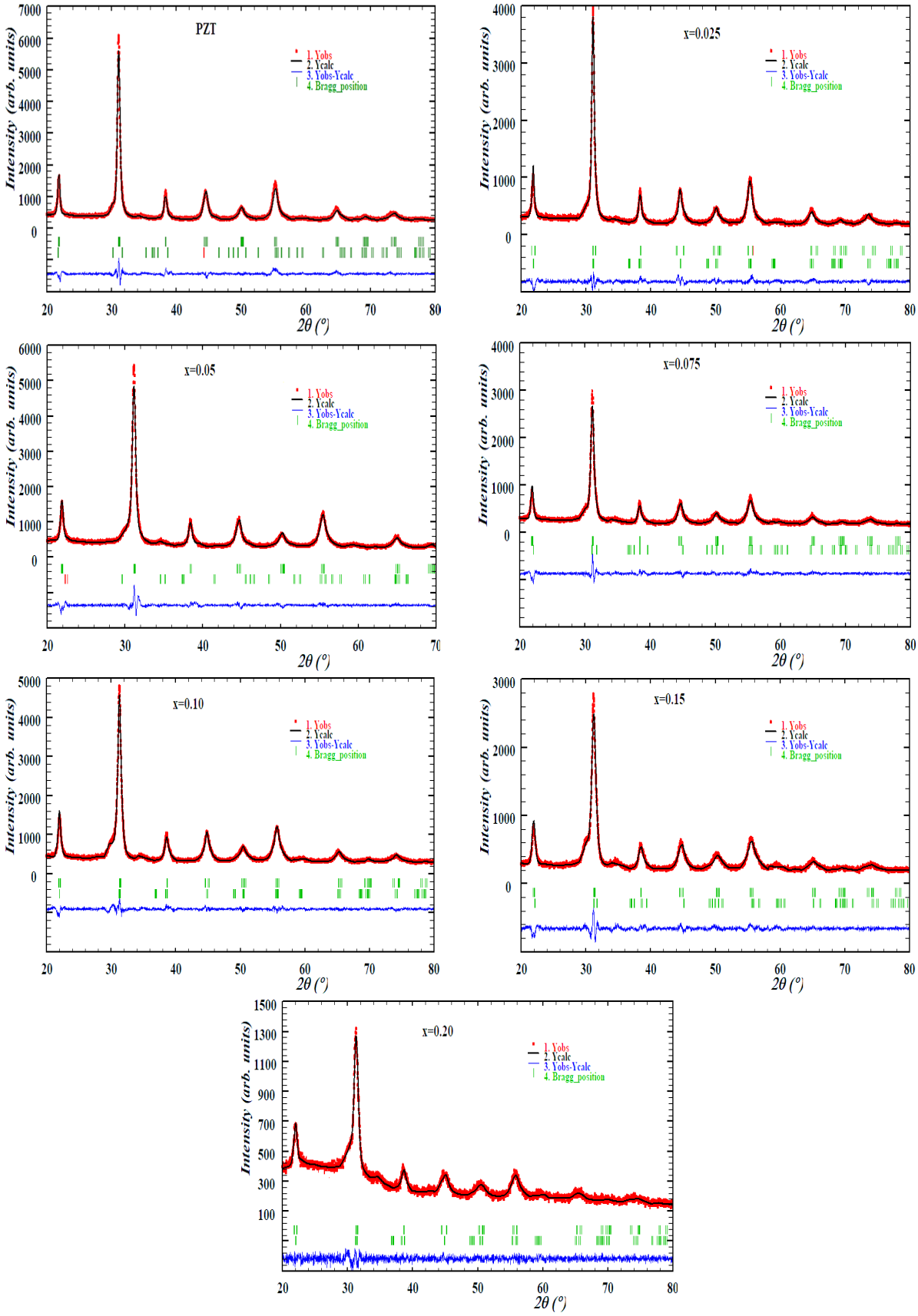

Fig. 2. Rietveld refined the XRD pattern for the PFZT samples calcined at 700°C/4h.

[DOI: 10.22068/ijmse.2938]

Also, the evolution of the percentage of phases shows a significant variation with the Fe content with a dominance of the tetragonal structure for all the samples, except 2.5% where the rhombohedral structure is present with more than 60%.

3.2. Raman Spectra

Fig. 3 shows the evolution of the Raman spectra of PFZT samples in the frequency range of 100-1000 cm^{-1}. For pure PZT, all Raman bands are broad and asymmetric, and we have observed six peaks at 110 cm^{-1}, 188 cm^{-1}, 266 cm^{-1}, 321 cm^{-1}, 470 cm^{-1}, and 525 cm^{-1} and three broad peaks at 606 cm^{-1}, 709 cm^{-1} and 730 cm^{-1}. These peaks are attributed to the A1(1TO), E(2TO), E + B1, A1(2TO), E(3TO), E(4TO), A1(3TO), E(4LO), and A1(3LO) modes, respectively. These results are in good agreement with the literature [6,37,38]. The A1(1TO) Raman mode observed around 110 cm^{-1} is associated with the vibration of Pb-O [39]. The tetragonal phase is represented by the two modes A1(2TO) and E(2TO), and the E+B1 mode confirms the existence of the two rhombohedral and tetragonal structures [39]. The E (3TO) (470 cm^{-1}) and A1 (3TO) (606 cm^{-1}) modes correspond to the bending of the O-Zr/Ti-O. The E(TO_2) and B1+E modes are related to the TiO_6 rotation, while the A1(3LO) mode is due to the Zr/Ti-O stretching of the oxygen octahedron [40]. On the other hand, for Fe-doped PZT samples, all the modes of pure PZT are present in the Raman spectra of the different compositions (PFZT) but we observed, that when the Fe content increases, a decrease in intensity and a shift of some peaks (like A1(2TO), A1(1TO)) towards low frequencies for some values of x and towards high frequencies for the others. In addition, a new band was detected around 900 cm^{-1} for x= 0.15 and x=0.20. This band can be attributed to the A1g mode which is due to the FeO_6 octahedra. This mode is found by researchers who substituted iron in $BaTiO_3$ of tetragonal structure and by others who studied the phase transition of $Bi_5Ti_3FeO_{15}$ material by Raman spectroscopy[41,42]. We can also notice that the intensity of the A1 (2TO) and A1 (1TO) bands decreased with the increase of the Fe rate. Furthermore, the intensity of the E (3TO), E (4TO), and A1 (3TO) modes decreases relatively when the Fe content increases. These results may be due to the distortion of Zr/TiO_6, probably caused by the substitution of Zr^{4+} / Ti^{4+} by Fe^{2+}, which is confirmed by the work of Hasitha Ganegoda [43]. The presence of E(2TO), B1 + E, E(3TO), A1(3TO), E(4LO), and A1(3LO) modes indicates the dominance of the tetragonal phase in all samples, which confirms the X-ray diffraction results. These bands are shifted towards low frequencies and others towards higher frequencies which can be due to the substitution of the Pb or Zr/Ti atom by another atom (Fe) confirming the variation in the fluctuation of the lattice parameters in the XRD.

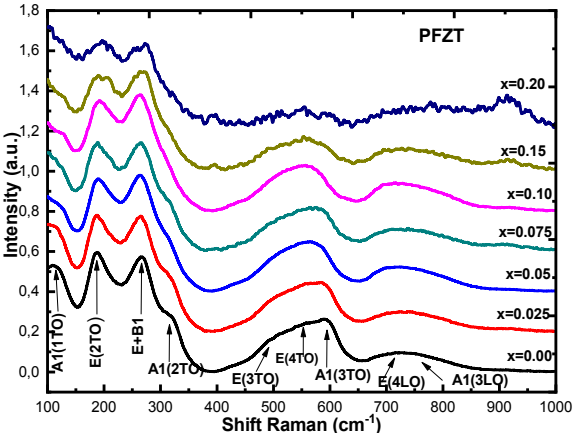

Fig. 3. Raman spectra of PFZT powders for x= 0.00, 0.025, 0.05, 0.075, 0.10, 0.15, 0.20.

3.3. SEM Results

The SEM micrographs for the PFZT ceramics sintered at 1100°C for 4 h are shown in figure 4. These images show that the morphology is well developed and the grains are homogeneous and regular in form with the presence of some pores. For x= 0.00 and 0.025 samples, the microstructure is characterized by grains of quasi-tetragonal form with the presence of small spherical grains. When the Fe content increases, the number of pores increases, and the ceramics are formed with a mixture of spherical grains. This indicates a new rearrangement of the structure. In addition, the average grain size changes with the change in the Fe content. Indeed, the values of the average grain size are presented in table 2. We notice that the average grain size of the undoped ceramic is about 3.45 µm which decreases and reaches a minimum value of 1.17 µm when the Fe content increases to 0.15. Furthermore, we have traced the evolution of the average grain size of PFZT ceramics as a function of Fe content as presented in figure 5.

[DOI: 10.22068/ijmse.2938]

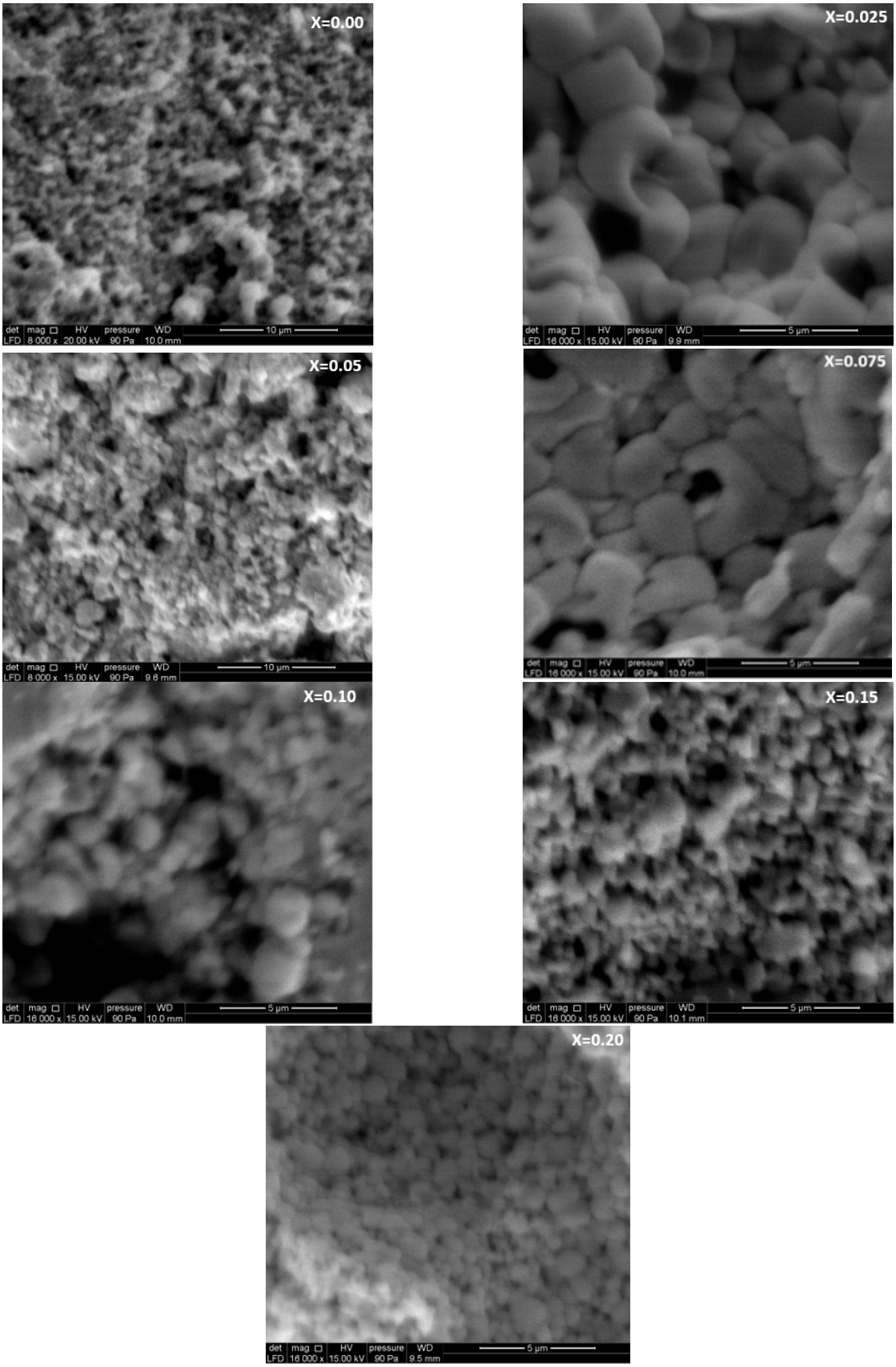

Fig. 4. SEM micrographs of PFZT ceramics for 0.00≤ x≤ 0.20 sintered at 1100°C for 4 h.

[DOI: 10.22068/ijmse.2938]

This figure shows a considerable decrease in the average grain size from 0.00 to 0.05 of the Fe ratio, then a rapid increase at x= 0.075. Beyond x= 0.075, the grain size decreases until x= 0.15 followed by an increase for x= 0.20. This evolution of the grain size is probably due to the substitution of Pb ions by Fe ions that decrease the lattice parameters found in XRD and so decrease also the grains size for doping ratios x= 0.00, 0.025, 0.05,0.10, and 0.15. While the increase in grain size for x= 0.075 is possibly due to the substitution of Ti/Zr ions by Fe^{2+}. These results are in good agreement with the XRD results presented previously.

Table 2. Average grain size of different composition of PFZT ceramics sintered at 1100°C.

Composition of Fe	Average grain size (µm)
x=0.00	3.45
x=0.025	3.20
x=0.05	1.26
x=0.075	3.51
x=0.10	1.60
x=0.15	1.17
x=0.20	1.28

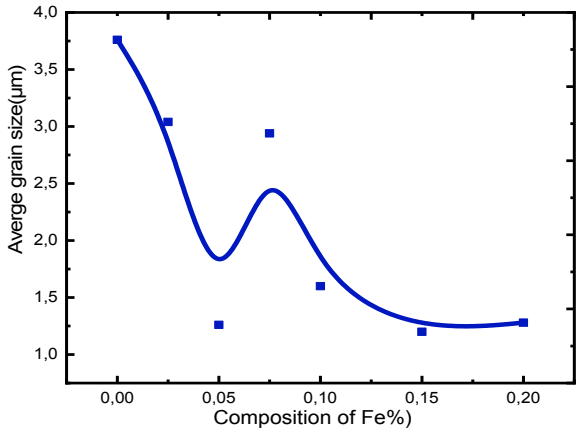

Fig. 5. Variation of grain size of PFZT ceramics sintered at 1100°C for 4 h.

3.4. Dielectric Properties

3.4.1. Dielectric constant (εr) as a function of temperature

Fig .6 shows the evolution of the dielectric constant of PFZT samples with (x= 0.00; 0.025; 0.05; 0.075; 0.10; 0.15 and 0.20) as a function of temperature at different frequencies. For the pure PZT (x= 0.00), the dielectric permittivity increases with increasing temperature and reaches a maximum at a temperature Tc= 410°C. This maximum is independent of the frequency from 50 to 900 kHz, it indicates the phase transition between the ferroelectric phase and the paraelectric phase at this temperature (Tc) [34, 35]. This result is confirmed by the literature [13, 45]. Similar behavior to pure PZT is observed for PFZT ceramic at x= 0.025 of Fe rate. While for other values of x the dielectric permittivity of PFZT samples (x= 0.05, 0.075, 0.010, 0.015, and 0.020) show the same behavior as pure PZT for frequencies ≤100KHz and the maximum of the dielectric constant is not observed at the limit temperature of measurement in the case of x= 0.075 and 0.010 which indicates the shift of the transition temperature towards the higher temperatures while it is shifted towards the lower temperatures for x= 0.025, 0.05, and 0.015 and 0.020, in where the transition peak is obtained. Furthermore, the maximum value of the dielectric permittivity (ε_{rmax}) shows a significant decrease for x= 0.025, then it increases beyond x= 0.025 and it remains almost constant for x >0.10 of Fe content. Fig.7 shows the variation of the dielectric constant with temperature for the PFZT ceramics at higher frequencies. For x= 0.00 and 0.025 and the frequencies f ≥1 MHz, the dielectric permittivity increases with increasing temperature and reaches a maximum, then decreases and reaches a minimum and increases thereafter. The maximum dielectric constant $\varepsilon_{r,max}$ moves towards the low temperatures when the frequency increases. This is the phenomenon of dielectric resonance [46, 28].

This behavior of the dielectric constant is observed for the other samples of different Fe concentrations but for frequencies f ≥500KHz. Table 8 shows the values of $\varepsilon_{r,max,}$ and T_m at three various frequencies 1 MHz, 1.4 MHz, and 1.8MHz. We observe that the maximum dielectric permittivity and the transition temperature increase as the frequency decreases. For all the tree frequencies, the value of Tm decreases with the increase in Fe concentration. While the value of $\varepsilon_{r,max}$ is minimal at x= 0.075 of Fe content.

3.5. Dielectric Constant as a Function of Frequency

The variation of dielectric permittivity as a function of frequency in the range of 100 Hz to 2 MHz at different temperatures for PFZT ceramics with (x= 0.0, 0.025, 0.05, 0.075, 0.10, 0.15 and 0.20) is shown in fig. 8.

[DOI: 10.22068/ijmse.2938]

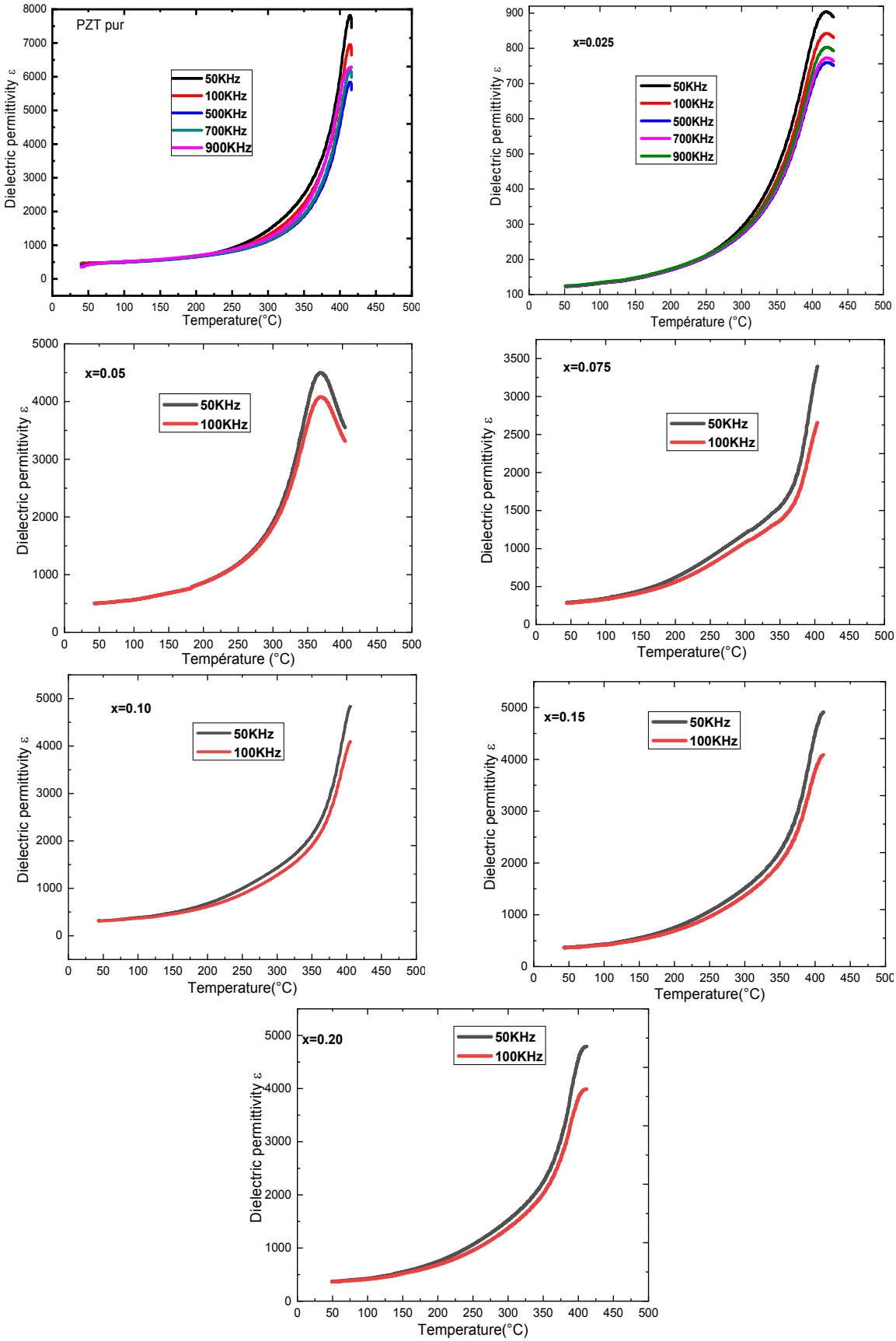

Fig. 6. Temperature dependence of dielectric permittivity at low frequencies of PFZT ceramics for 0.00≤ x≤0.20.

[DOI: 10.22068/ijmse.2938]

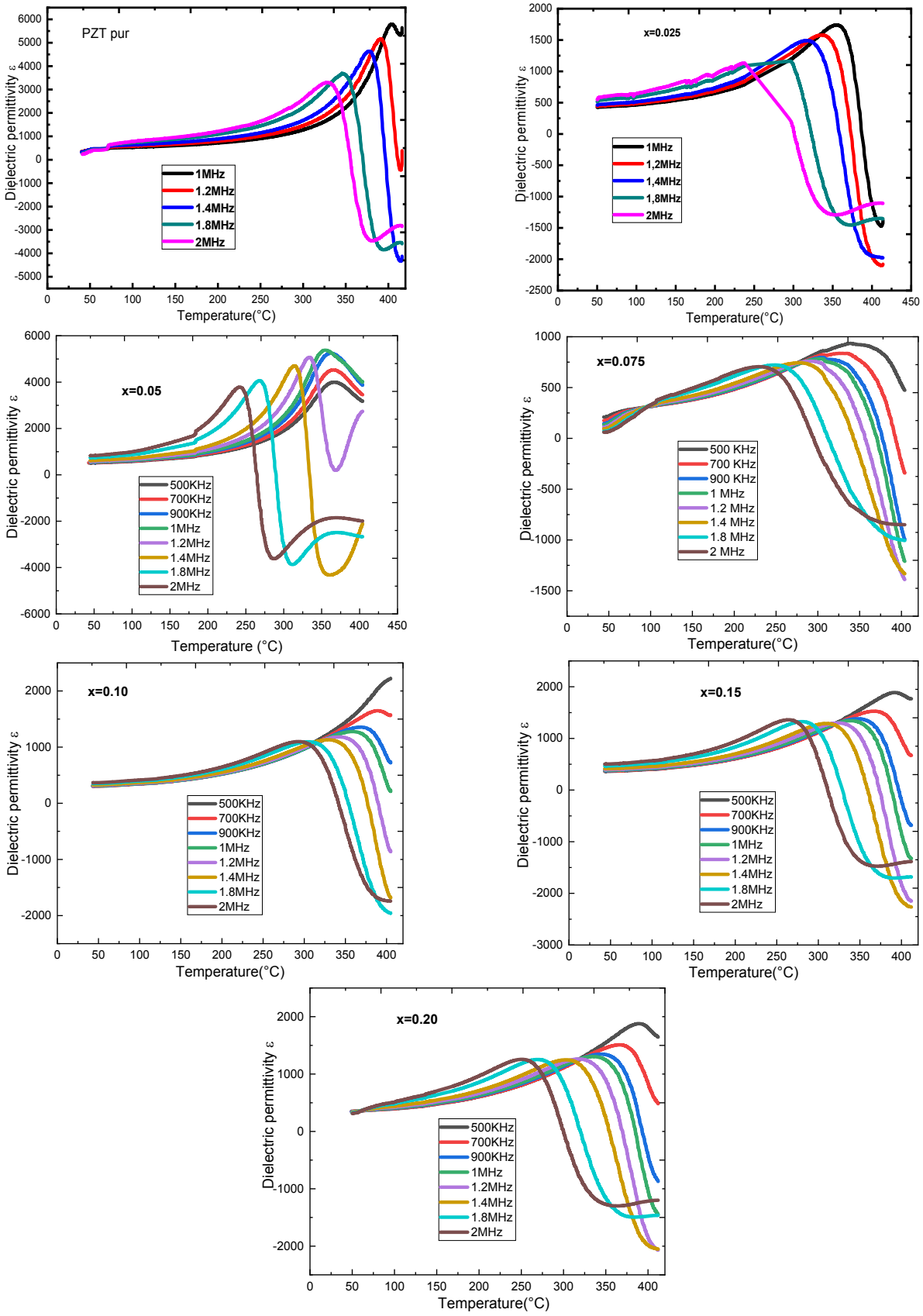

Fig. 7. Temperature dependence of dielectric permittivity at higher frequencies of PFZT ceramics for $0.00 \leq x \leq 0.20$.

[DOI: 10.22068/ijmse.2938]

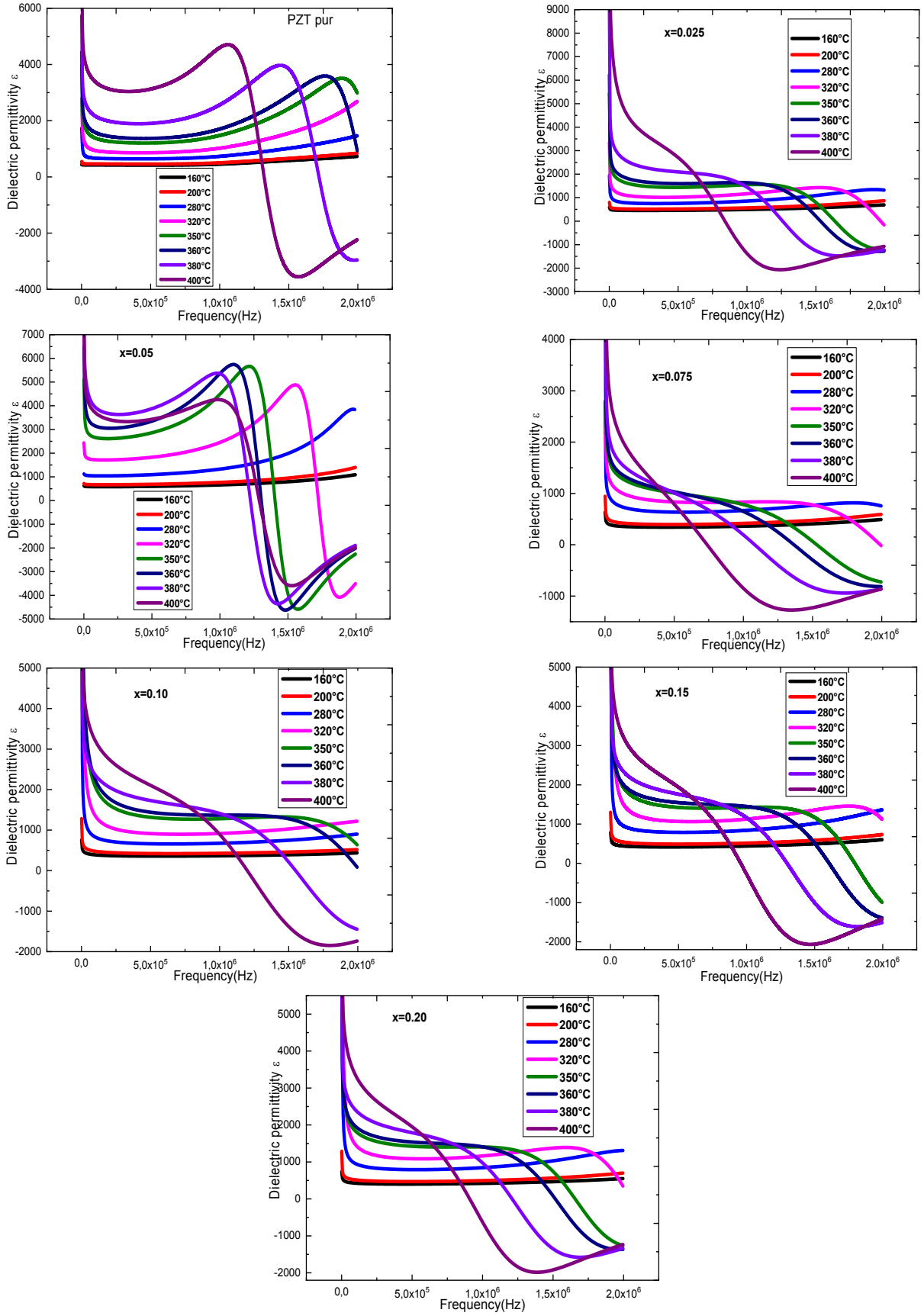

Fig. 8. Dielectric constant variation as a function of frequency at different temperatures for PFZT samples.

[DOI: 10.22068/ijmse.2938]

Table 3. Dielectric constant $\varepsilon_{r\ max}$, Tc, and Tm at different frequencies of PFZT samples.

Frequencies	1 MHz		1.4 MHz		1.8 MHz	
x	Tm	$\varepsilon_{r\ max}$	Tm	$\varepsilon_{r\ max}$	Tm	$\varepsilon_{r\ max}$
x= 0.00	402	5877	377	4640	344	3787
x= 0.025	351	1760	316	1514	297	1178
x= 0.05	353	5383	312	4711	266	4071
x= 0.075	294	796	277	759	243	734
x= 0.10	355	1288	328	1154	300	1115
x= 0.15	333	1486	308	1310	279	1352
x= 0.20	330	1450	301	1256	267	1256

For the pure PZT, the dielectric permittivity decreases at low frequencies and then becomes almost constant up to 5.10^5 Hz, which is typical of classical ferroelectrics. For temperatures higher than 320°C, the dielectric permittivity increases with the increase of the frequency and reaches a maximum value corresponding to the resonance frequency (fr) then it decreases rapidly for a frequency called antiresonance (fa). For temperatures under 320°C, the maximum dielectric constant can be observed for frequencies above 2 MHz. The resonant frequency increases with increasing temperature and shifts to the lower frequencies. These results are in good agreement with the literature [47, 48]. The same behavior as pure PZT was found for x= 0.05 but from 380°C the maximum of the dielectric permittivity shifts to high frequencies when the temperature increases suggesting dielectric relaxation [42]. For the other samples, the dielectric permittivity decreases rapidly with increasing frequency and the maximum value becomes lower compared with x= 0.00 and x= 0.05. At low frequencies, the high dielectric permittivity is attributed to the existence of space charge polarization at the grain boundaries, which creates a potential barrier, causing a high value of the dielectric constant.

4. CONCLUSIONS

In summary, The $Pb_{(1-x)}Fe_x(Zr_{0.52}Ti_{0.48})O_3$ (PFZT) ceramics with compositions ($0\leq x\leq 20\%$)_was prepared by the sol-gel method. The result of the X-ray diffraction study showed the formation of the crystalline structure without any trace of the secondary phase. Besides, the Rietveld refinement method confirmed the coexistence of rhombohedral and tetragonal phases. The Raman spectra of pure PZT powder showed the presence of eight peaks attributed to the tetragonal and rhombohedral bands. While for Fe-doped samples, we showed the disappearance of some peaks observed in pure PZT. The SEM micrographs of PFZT samples indicated the decrease of the grain size when Fe content increases and the number of pores was increased. The dielectric measurements as a function of temperature indicated that the dielectric permittivity was minimal at x= 0.075 while the transition temperature was decreased with increasing the Fe concentration in PZT ceramic until x= 0.075 and then it was increased. The phenomenon of resonance dielectric was obtained from the variation of dielectric permittivity as a function of frequency.

REFERENCES

[1]. M. Siddiqui, J. J. Mohamed, and Z. A. Ahmad, "Structural, piezoelectric, and dielectric properties of PZT-based ceramics without excess lead oxide," J. Aust. Ceram. Soc., vol. 56, no. 2, pp. 371–377, 2020, doi: 10.1007/s41779-019-00337-3.

[2]. N. Banerjee, G. Koster, and G. Rijnders, "Submicron patterning of epitaxial $PbZr_{0.52}Ti_{0.48}O_3$ heterostructures," Appl. Phys. Lett., vol. 102, no. 14, pp. 0–5, 2013, doi: 10.1063/1.4801776.

[3]. S. Nayak, T. Kumar, and D. Khastgir, "permittivity : Switchable dielectric phase transition with temperature," Ceram. Int., vol. 42, no. 13, pp. 14490–14498, 2016, doi: 10.1016/j.ceramint.2016.06.056.

[4]. R. N. Perumal, S. Sadhasivam, and V. Athikesavan, "Structural, dielectric, AC conductivity, piezoelectric and impedance spectroscopy studies on $PbZr_{0.52}Ti_{0.48}O_3$:Re^{3+}(Re^{3+}: La^{3+}, Nd^{3+} and Dy^{3+}) ceramics," Results Phys., vol. 15, no. November 2018, p. 102729, 2019, doi:

[DOI: 10.22068/ijmse.2938]

10.1016/j.rinp.2019.102729.

[5]. M. Kumar, S. Shankar, S. Kumar, O. P. Thakur, and A. K. Ghosh, "Structural, magnetic, dielectric and magneto-dielectric coupling analysis of ferromagnetic-$PbZr_{0.52}Ti_{0.48}O_3$ nanocomposites," J. Mater. Sci. Mater. Electron., vol. 27, no. 7, pp. 6849–6853, 2016, doi: 10.1007/s10854-016-4637-8.

[6]. M. Ahabboud, T. Lamcharfi, F. Abdi, N. Hadi, F. Z. Ahjyaje, and M. Haddad, "Effect of Cu Doping on Structural and Dielectric Properties of $Pb_{1-x}Cu_x(Zr_{0.52}Ti_{0.48})O_3$ (PCx ZT) ($0 \leq x \leq 0.2$) Ceramics Prepared by Sol-Gel Method M.," Asian J. Chem., vol. 30, no. 18, pp. 2424–2430, 2018.

[7]. H. L. Huang, G. Z. Cao, and I. Y. Shen, "Hydrothermal synthesis of lead zirconate titanate (PZT or $Pb(Zr_{0.52}Ti_{0.48})O_3$) nano-particles using controlled ramping and cooling rates," Sensors Actuators, A Phys., vol. 214, pp. 111–119, 2014, doi: 10.1016/j.sna.2014.04.018.

[8]. F. Gheorghiu, R. Apetrei, M. Dobromir, A. Ianculescu, D. Luca, and L. Mitoseriu, "Investigation of Co-doped PZT films deposited by rf-magnetron sputtering," Process. Appl. Ceram., vol. 8, no. 3, pp. 113–120, 2014, doi: 10.2298/PAC1403113G.

[9]. M. Khajelakzay and E. Taheri-Nassaj, "Synthesis and characterization of $Pb(Zr_{0.52}Ti_{0.48})O_3$ nanofibers by electrospinning, and dielectric properties of PZT-Resin composite," Mater. Lett., vol. 75, pp. 61–64, 2012, doi: 10.1016/j.matlet.2012.01.082.

[10]. L. Jin, "Broadband Dielectric Response in Hard and Soft PZT," vol. 4988, 2011, http://infoscience.epfl.ch/record/162134.

[11]. Y. H. Paik, H. S. Kojori, and S. J. Kim, "Ferroelectric devices using lead zirconate titanate (PZT) nanoparticles," Nanotechnology, vol. 27, no. 7, p. 75204, 2016, doi: 10.1088/0957-4484/27/7/075204.

[12]. E. Nogas-Ćwikiel, "Fabrication of Mn doped PZT for ceramic-polymer composites," Arch. Metall. Mater., vol. 56, no. 4, pp. 1065–1069, 2011, doi: 10.2478/v10172-011-0118-5.

[13]. R. Rai, S. Sharma, N. C. Soni, and R. N. P. Choudhary, "Investigation of structural and dielectric properties of (La, Fe)-doped PZT ceramics," Phys. B Condens. Matter, vol. 382, no. 1–2, pp. 252–256, 2006, doi: 10.1016/j.physb.2006.02.024.

[14]. A. Hizebry, "Propagation de Fisuures Danns les Céramiques Piezo-Electriques De Type PZT : Effets De Dopage au Potassium et Au Niobium," no. May, pp. 1–142, 2007.

[15]. C. A. Oliveira, E. Longo, J. A. Varela, and M. A. Zaghete, "Synthesis and characterization of lead zirconate titanate (PZT) obtained by two chemical methods," Ceram. Int., vol. 40, no. 1 part B, pp. 1717–1722, 2014, doi: 10.1016/j.ceramint.2013.07.068.

[16]. B. Noheda, J. Gonzalo, L. Cross, R. Guo, and S. Park, "Tetragonal-to-monoclinic phase transition in a ferroelectric perovskite: The structure," Phys. Rev. B - Condens. Matter Mater. Phys., vol. 61, no. 13, pp. 8687–8695, 2000, doi: 10.1103/PhysRevB.61.8687.

[17]. T. Kimura, T. Goto, H. Shintani, K. Ishizaka, T. Arima, and Y. Tokura, "Magnetic control of ferroelectric polarization," Nature, vol. 426, no. 6962, pp. 55–58, 2003, doi: 10.1038/nature02018.

[18]. M. Fiebig, T. Lottermoser, D. Fröhlich, A. V. Goltsev, and R. V. Pisarev, "Observation of coupled magnetic and electric domains," Nature, vol. 419, no. 6909, pp. 818–820, 2002, doi: 10.1038/nature01077.

[19]. W. Eerenstein, N. D. Mathur, and J. F. Scott, "Multiferroic and magnetoelectric materials," Nature, vol. 442, no. 7104, pp. 759–765, 2006, doi: 10.1038/nature05023.

[20]. J. S. Almeida, "The Emergence of the ERC," Science (80-.)., vol. 307, no. 5713, pp. 1200–1200, 2005, doi: 10.1126/science.307.5713.1200b.

[21]. C. W. Nan, M. I. Bichurin, S. Dong, D. Viehland, and G. Srinivasan, "Multiferroic magnetoelectric composites: Historical perspective, status, and future directions," J. Appl. Phys., vol. 103, no. 3, 2008, doi: 10.1063/1.2836410.

[22]. K. K. Patankar, S. A. Patil, K. V.

[DOI: 10.22068/ijmse.2938]

Sivakumar, R. P. Mahajan, Y. D. Kolekar, and M. B. Kothale, "AC conductivity and magnetoelectric effect in $CuFe_{1.6}Cr_{0.4}O_4$-$BaTiO_3$ composite ceramics," Mater. Chem. Phys., vol. 65, no. 1, pp. 97–102, 2000, doi: 10.1016/S0254-0584(00)00216-9.

[23]. K. Mori and M. Wuttig, "Magnetoelectric coupling in Terfenol-D/polyvinylidenedifluoride composites," Appl. Phys. Lett., vol. 81, no. 1, pp. 100–101, 2002, doi: 10.1063/1.1491006.

[24]. J. Ryu, A. V. Carazo, K. Uchino, and H. E. Kim, "Magnetoelectric properties in piezoelectric and magnetostrictive laminate composites," Japanese J. Appl. Physics, Part 1 Regul. Pap. Short Notes Rev. Pap., vol. 40, no. 8, pp. 4948–4951, 2001, doi: 10.1143/jjap.40.4948.

[25]. S. Dong, J. Zhai, J. Li, and D. Viehland, "Small dc magnetic field response of magnetoelectric laminate composites," Appl. Phys. Lett., vol. 88, no. 8, pp. 29–31, 2006, doi: 10.1063/1.2178582.

[26]. S. Dong, J. Zhai, J. F. Li, and D. Viehland, "Magnetoelectric effect in Terfenol-D/Pb(Zr, TiO) $_3$/μ-metal laminate composites," Appl. Phys. Lett., vol. 89, no. 12, pp. 21–24, 2006, doi: 10.1063/1.2355459.

[27]. E. Pakizeh, "Optical response and structural properties of Fe-doped $Pb(Zr_{0.52}Ti_{0.48})O_3$ nanopowders," J. Mater. Sci. Mater. Electron., vol. 31, no. 6, pp. 4872–4881, 2020, doi: 10.1007/s10854-020-03050-1.

[28]. M. Ahabboud, M. Amarass, F.Z. A, F. Abdi, and T. Lamcharfi, "Structural and dielectric properties of Pb $(Zr_{0.52}\ Ti_{0.48})_{1-3x/4}Fe_x\ O_3$ ceramics at $0\leq x\leq 0.20$ prepared by sol-gel method," IOP Conf. Ser. Mater. Sci. Eng., pp. 1–3, 2021, doi: 10.1088/1757-899X/1160/1/012001.

[29]. R. Rai, S. Sharma, and R. N. P. Choudhary, "Dielectric and piezoelectric studies of Fe doped PLZT ceramics," Mater. Lett., vol. 59, no. 29–30, pp. 3921–3925, 2005, doi: 10.1016/j.matlet.2005.07.034.

[30]. N. Kumari et al., Multifunctional behavior of acceptor-cation substitution at the higher doping concentration in PZT ceramics, vol. 45, no. 10. 2019.

[31]. S. R. Sangawar, B. Praveenkumar, P. Divya, and H. H. Kumar, "Fe Doped Hard PZT Ceramics for High Power SONAR Transducers," Mater. Today Proc., vol. 2, no. 4–5, pp. 2789–2794, 2015, doi: 10.1016/j.matpr.2015.07.279.

[32]. S. Samanta, V. Sankaranarayanan, and K. Sethupathi, "Effect of Successive Multiple Doping of La, Nb and Fe on Structure and Lattice Vibration of MPB PZT," Mater. Today Proc., vol. 5, no. 14, pp. 27919–27927, 2018, doi: 10.1016/j.matpr.2018.10.031.

[33]. A. K. Zak, "Synthesis and characterization of sol-gel derived single-phase PZT nanoparticles in aqueous polyol solution," vol. 88, no. August 2010.

[34]. H. Li, J. Liu, H. Yu, and S. Zhang, "Relaxor behavior and Raman spectra of CuO-doped $Pb(Mg_{1/3}Nb_{2/3})O_3$-$PbTiO_3$ ferroelectric ceramics," J. Adv. Ceram., vol. 3, no. 3, pp. 177–183, 2014, doi: 10.1007/s40145-014-0106-0.

[35]. R. Ranjan, R. Kumar, B. Behera, and R. N. P. Choudhary, "Effect of Sm on structural, dielectric and conductivity properties of PZT ceramics," Mater. Chem. Phys., vol. 115, no. 1, pp. 473–477, 2009, doi: 10.1016/j.matchemphys.2009.01.017.

[36]. Bouzid and Abderrazak, "Contribution à la compréhension des phénomènes de dissipation d'énergie dans les céramiques piézo-électriques de type PZT : Effets du dopage au potassium et au niobium," 2002.

[37]. E. Buixaderas, M. Berta, L. Kozielski, and I. Gregora, "Phase Transitions : A Multinational Raman spectroscopy of Pb $(Zr_{1-x}Ti_x)\ O_3$ graded ceramics around the morphotropic phase boundary," Phase Transitions, no. July 2013, pp. 37–41, doi: 10.1080/01411594.2011.552049.

[38]. M. Deluca et al., "Raman spectroscopic study of phase transitions in undoped morphotropic $PbZr_{1-x}Ti_xO_3$," J. Raman Spectrosc., vol. 42, no. 3, pp. 488–495, 2011, doi: 10.1002/jrs.2714.

[39]. P. Kour, S. K. Pradhan, P. Kumar, S. K. Sinha, and M. Kar, "Enhanced ferroeletric and piezoelectric properties of Nd^{3+} doped PZT nanoceramics," AIP Conf. Proc., vol. 1728, pp. 3–7, 2016, doi:

[DOI: 10.22068/ijmse.2938]

10.1063/1.4946541.
[40]. D. A. Sanchez et al., "Symmetries and multiferroic properties of novel room-temperature magnetoelectrics: Lead iron tantalate - Lead zirconate titanate (PFT/PZT)," AIP Adv., vol. 1, no. 4, pp. 0–14, 2011, doi: 10.1063/1.3670361.
[41]. M. Bian et al., "Phase transition of $Bi_5Ti_3FeO_{15}$ ceramics discovered by Raman spectroscopy and in situ synchrotron XRD under stress field," Appl. Phys. Lett., vol. 117, no. 2, 2020, doi: 10.1063/5.0019034.
[42]. N. Gouitaa, T. Lamcharfi, M. F. Bouayad, F. Abdi, N. S. Echatoui, and N. Hadi, "Dielectric anomalies of $BaTi_{1-x}Fe_xO_3$ ceramics for x= 0.0 to 0.6 of Fe doping concentration," Asian J. Chem., vol. 29, no. 10, pp. 2143–2148, 2017, doi: 10.14233/ajchem.2017.20653.
[43]. H. Ganegoda et al., "Role of Fe Doping on Local Structure and Electrical and Magnetic Properties of $PbTiO_3$," J. Phys. Chem. C, vol. 125, no. 22, pp. 12342–12354, 2021, doi: 10.1021/acs.jpcc.1c02297.
[44]. A. Gupta and R. Chatterjee, "Study of dielectric and magnetic properties of $PbZr_{0.52}Ti_{0.48}O_3$-$Mn_{0.3}Co_{0.6}Zn_{0.4}Fe_{1.7}O_4$ composite," J. Magn. Magn. Mater., vol. 322, no. 8, pp. 1020–1025, 2010, doi: 10.1016/j.jmmm.2009.12.007.
[45]. E. M. B. Ourim, H. T. Anaka, M. G. Abbay, and G. F. Antozzi, "Internal Friction and Dielectric Measurements in Lead Zirconate Titanate Ferroelectric Ceramics," Jpn. J. Appl. Phys, vol. 5542, 2000.
[46]. T. Lamcharfi et al., "Dielectric and relaxation studies in hydrothermal processed PLZT ceramics," vol. 6, no. 1, pp. 76–82, 2005.
[47]. M. Mesrar, "Effect of barium doping on electrical and electromechanical," Mediterr. J. Chem., vol. 8, no. 2, pp. 198–208, 2019.
[48]. A. El Basset, "Synthèse et Caractérisation de matériaux de Titanate de Baryum purs et dopés au Strontium et au Zirconium," FST, usmba Fès, 2014.

[DOI: 10.22068/ijmse.2938]